Journal of
INTERNATIONAL MEDICAL RESEARCH

Effects of donor age on human adipose-derived adherent stromal cells under oxidative stress conditions

Sang Woo Kim[1,2,*], Jung-Won Choi[2,3,*],
Chang Youn Lee[4], Jiyun Lee[5], Sunhye Shin[4],
Soyeon Lim[1,2], Seahyoung Lee[1,2],
Il-Kwon Kim[2,6], Hoon-Bum Lee[7,#] and
Ki-Chul Hwang[1,2,#]

Abstract

Objective: Adipose-derived stromal vascular fractions (SVFs) are heterogeneous complex populations of cells with therapeutic efficacy for tissue generation and vascular stabilization. SVFs have cardiomyogenic potential, and many researchers have examined the possibility of SVF transplantation for heart disease. In cell-based therapies, donor age affects the regenerative capability, cell yield, and differentiation potential of adult tissues; however, opposing or controversial results have been found in humans. We examined whether SVF transplantation into impaired heart tissue shows differential effects according to donor age.

Methods: We investigated differences in protein expression in human umbilical vein endothelial cells (HUVECs) co-cultured with adipose-derived adherent stromal cells (ADASs) from donors of different ages [>40-year-olds (40s group) and >60-year-olds (60s group)] under oxidative stress conditions.

[1]Catholic Kwandong University, International St. Mary's Hospital, Incheon Metropolitan City, Republic of Korea
[2]Institute for Bio-Medical Convergence, College of Medicine, Catholic Kwandong University, Gangneung-si, Gangwon-do, Republic of Korea
[3]Department of Health and Environment, College of Engineering, Catholic Kwandong University, Gangneung-si, Gangwon-do, Republic of Korea
[4]Department of Integrated Omics for Biomedical Sciences, Graduate School, Yonsei University, Seoul, Republic of Korea
[5]Brain Korea 21 PLUS Project for Medical Science, Yonsei University College of Medicine, Seoul, Republic of Korea

[6]Cell Therapy Center, Catholic Kwandong University, International St. Mary's Hospital, Incheon Metropolitan City, Republic of Korea
[7]Department of Plastic and Reconstructive Surgery, Catholic Kwandong University, International St. Mary's Hospital, Incheon Metropolitan City, Republic of Korea

[*]These authors contributed equally to this work.
[#]These authors contributed equally to this work.

Corresponding author:
Ki-Chul Hwang, Catholic Kwandong University, International St. Mary's Hospital, Incheon Metropolitan City 22711, Republic of Korea.
Email: kchwang@cku.ac.kr

Results: Although co-culturing HUVECs with ADASs ameliorated inflammation due to increased oxidative stress conditions, few differences were observed between the ADASs from the 40s and 60s groups. Moreover, the Database for Annotation, Visualization, and Integrated Discovery classification tool revealed differentially expressed genes in the Kyoto Encyclopedia of Genes and Genomes pathway associated with cytokine–cytokine receptor interaction in response to ADASs.

Conclusion: Protein expression profiles were unchanged in HUVECs induced by isolated ADASs from donors of different ages under oxidative stress conditions.

Introduction

Adipose tissue is a rich source of cells with prospects for tissue engineering and regenerative medicine.[1,2] Adipose-derived stromal vascular fractions (SVFs) contain adipose-derived stem cells (ASCs), endothelial (progenitor) cells, vascular smooth muscle cells, mesenchymal stem cells (MSCs), fibroblasts, macrophages, and pericytes, all of which exhibit mesodermal and ectodermal capacity.[3,4] This heterogeneous complex population has shown efficacy in tissue generation and vascular stabilization[3,4] as well as substantial potential for therapeutic applications in lipotransfer, management of diabetes-related complications, nerve regeneration, burn wound therapy, and other uses.[1,2] In particular, SVFs also have cardiomyogenic potential,[5] and many research groups are studying the possibility of SVF transplantation as a therapy for heart disease.[3,6–8] ASCs improve cardiac function and perfusion after acute and chronic myocardial infarction in the rodent and pig,[3,6,7] and their transplantation has been suggested as a useful therapeutic option for angiogenesis in chronic ischemic heart disease.[8] Despite these attractive advantages of SVFs in clinical interventions, their use in many diseases has not been fully evaluated in clinical studies.[9]

Donor age is known to affect the regenerative capability of adult tissues in cell-based therapies; donor age also affects the number of adipose-derived MSCs, cell yield of the SVF, and differentiation potential and angiogenic functional capacity of adipose tissue.[10–12] However, controversial results have been shown in humans.[13–16] Researchers have found that adipose-derived MSCs exhibit similar osteogenic paracrine activity in all age groups of donors.[13] No correlation has been shown between the cell yield of ASCs from liposuction aspirates and donor age,[14] and the age of the donor does not affect the proliferation and differentiation capacities of cultured ASCs.[15] In addition, one study showed that the effect of autologous SVF transplantation for rheumatoid arthritis was unrelated to donor age.[16]

Therefore, to clarify the above discrepancies in previous research, we performed the present study to determine whether SVF transplantation into impaired heart tissue shows differential effects according to donor age. We investigated the differences in protein expression in human

umbilical vein endothelial cells (HUVECs) co-cultured with adipose-derived adherent stromal cells (ADASs) from individuals of different ages under oxidative stress conditions due to an abundant number of endothelial cells in the heart.[17] This study was based on the concept that redox signaling influences many physiological processes in the heart and plays a critical role in pathological cardiac remodeling.[18]

Materials and methods

Donors and adipose tissue harvesting

Human adipose tissue samples for isolation of SVFs were obtained from donors recruited at International St. Mary's Hospital of Catholic Kwandong University. All patients provided verbal informed consent to participate. The study protocol was approved by the ethics review committee of the Institutional Review Board, College of Medicine, Catholic Kwandong University. Liposuction was performed from the abdominal wall by gentle manual techniques under general anesthesia and sterile conditions. In all cases, the fat was harvested from the abdominal wall by gentle manual techniques.

Isolation of SVFs and culture of ADASs

SVFs were isolated from human adipose tissue samples by an enzymatic digestion method using the SmartX kit (DongKoo Bio & Pharma Co., Seoul, South Korea) following the manufacturer's instructions. Briefly, adipose tissue was centrifuged at $1,700 \times g$ for 5 min to remove water, tumescent solution, and oil. Next, 50 ml of fat tissue was digested with 0.075% collagenase type I at 37°C for 30 min under gentle agitation. After the digested tissue was filtered through a 75-µm strainer to remove residual tissue, the cell suspension was centrifuged

and washed three times with phosphate-buffered saline (PBS) (HyClone, Logan, UT, USA). Total and live cell counts were performed using the NucleoCounter® NC-200™ automated cell counter (ChemoMetec, Allerød, Denmark). The SVFs were cultured in 10% fetal bovine serum (HyClone)–supplemented Dulbecco's Modified Eagle's Media (HyClone) and 1% penicillin/streptomycin at a density of 5×10^4 cells/cm^2 in a 100-mm dish in a humidified atmosphere with 5% CO_2 at 37°C. After plating on culture dishes, non-adherent cells were discarded by changing the culture medium and ADASs passaged three times.

HUVEC culture

HUVECs (Lonza, Walkersville, MD, USA) were cultured in Clonetics Endothelial Growth Basal Medium 2 (Lonza) supplemented with Clonetics Endothelial Growth Medium 2 SingleQuots (Lonza) using dishes and plates coated with 0.1% gelatin (BD, Sparks, MD, USA) in a humidified atmosphere of 5% CO_2 and 95% air at 37°C.

Cell viability assay

Cell viability was measured using Ez-Cytox (Daeillab Service, Seoul, Korea). HUVECs were seeded 24 h prior to H_2O_2 treatment at a density of 5×10^4 cells/cm^2 onto a 96-well plate. After 24 h, H_2O_2 (0, 10, 20, 30, 40, or 50 µM) was applied to the HUVECs for 2, 4, or 6 h. After the addition of 10 µL of Ez-Cytox into each well, cell viability was evaluated by measuring the optical density at 450 nm.

Reactive oxygen species detection assay

Reactive oxygen species (ROS) production in H_2O_2-treated HUVECs was assessed according to the levels of bright green-colored 2′,7′-dichlorofluorescein (DCF)

produced by the oxidation of DCF diacetate (DCF-DA) dye. The HUVECs were plated 24 h prior to H_2O_2 treatment at a density of 5×10^4 cells/cm^2 in a 6-well plate and washed twice with PBS after 24 h. ROS generation was induced in HUVECs after 2, 4, or 6 h of treatment with 0 to 50 µM H_2O_2, followed by incubation with 50 µM DCF-DA (Sigma-Aldrich, St. Louis, MO, USA) for 30 min in the dark at 37°C. The green fluorescence was detected by flow cytometry using a BD Accuri^{TM} C6 Cytometer (BD Biosciences, Piscataway, NJ, USA).

Co-culture of ADASs and HUVECs

HUVECs at passage 5 were plated 24 h prior to H_2O_2 treatment at a density of 5×10^4 cells/cm^2 in a 6-well plate and then treated with or without 40 µM H_2O_2 for 4 h. After 4 h, the cells were co-cultured with individual ADASs at passage 3 using trans-well inserts with a 0.4-µm porous translucent polyethylene terephthalate membrane (Falcon; Corning Life Sciences, Pittston, PA, USA) at a cell density identical to that of the HUVECs. Following co-culture for 24 or 48 h after the incubation period, the cells in the lower well were then harvested for further analysis. The experimental groups were designed as follows: Group 1 (negative control), HUVECs (monoculture); Group 2 (H_2O_2), HUVECs (monoculture) + H_2O_2; Groups 3, 4, and 5 (40s group), HUVECs and ADASs (40s group #1, #2 or #3, co-culture) + H_2O_2; and Groups 6, 7, and 8 (60s group), HUVECs and ADASs (60s group #1, #2, or #3, co-culture) + H_2O_2.

Flow cytometry

For the flow cytometric analysis, cells were collected using Accutase Cell Detachment Solution (Thermo Fisher Scientific, Waltham, MA, USA). The cells (5×10^5 cells/50 µL)

were incubated for 1 h with antibodies to CD31, CD34, CD45, CD90, CD105, CD106, or isotype control (Santa Cruz Biotechnology, Santa Cruz, CA, USA) on ice and then washed three times with PBS containing 2.5% fetal bovine serum and 0.1% sodium azide (Sigma-Aldrich; washing solution). The cells were further incubated for 1 h with fluorescein isothiocyanate-conjugated anti-mouse IgG or anti-rabbit IgG (Santa Cruz Biotechnology) on ice in the dark. The cells were then washed three times and analyzed via flow cytometry using a BD Accuri^{TM} C6 Cytometer (BD Biosciences).

Immunoblot analysis

The immunoblot analysis was performed according to the normalized methods of our previous studies.[19] Primary polyclonal antibody (Santa Cruz Biotechnology) and secondary antibodies (horseradish peroxidase-conjugated anti-goat IgG, anti-mouse IgG or anti-rabbit IgG; Santa Cruz Biotechnology) were used for detection of proteins of interest. The results were visualized using an enhanced chemiluminescence (ECL, Western Blotting Detection kit, GE Healthcare, Sweden) system, and the band intensities were quantified using ImageJ software.

RNA isolation, reverse-transcription polymerase chain reaction (PCR), and quantitative real-time PCR (qPCR)

Total RNA was isolated from HUVECs using TRIzol Reagent Solution (Life Technologies, Frederick, MD, USA) according to the manufacturer's instructions. Oligo dT-primed cDNA was synthesized from total RNA using the Maxime RT PreMix kit (iNtRON Biotechnology, Seongnam, Korea). The level of each gene transcript was quantitatively determined by qPCR using a StepOnePlus real-time PCR

system (Applied Biosystems, Foster City, CA, USA) with the SYBR Green Dye system [SYBR Premix Ex Taq (Tli RNase H Plus) and ROX reference dye (Takara Bio Inc., Foster City, CA, USA)]. The transcript level of each gene was normalized to the GAPDH transcript levels. Primers were designed using Primer3 and BLAST, and the primer set sequences are listed in Table 1.

Network analysis

For the gene/protein network analyses, targets identified in this study were analyzed using GeneMANIA (http://www.genemania.org) and the Database for Annotation, Visualization, and Integrated Discovery (DAVID).[20,21] DAVID provides a comprehensive set of functional annotation tools to interpret the biological relevance of such a large list of genes/proteins, whereas the GeneMANIA interface generates a list of genes with functional similarity based on the available genomics and proteomics information in the database. The GeneMANIA algorithm contains two integral parts: 1) a linear regression-based algorithm for calculating a single, composite functional association network from

Table 1. Sequences of primers used for quantitative real-time polymerase chain reaction

Genes		Primer sequence (5′-3′)
IL6	F	TCAATATTAGAGTCTCAACCCCCA
	R	GTTCATAGCTGGGCTCCTGG
IL8	F	CCACCGGAGCACTCCATAAG
	R	GTGAGATGGTTCCTTCCGGT
IFNG	F	TGAATGTCCAACGCAAAGCA
	R	CTGGGATGCTCTTCGACCTC
TNF	F	CACCACTTCGAAACCTGGGA
	R	TGTAGGCCCCAGTGAGTTCT
FGF1	F	GGGGTTGCTTAGAGCTGTGT
	R	GGAGCCAAGAATGTCAGCCT
FGF2	F	TCCACCTATAATTGGTCAAAGTGGT
	R	CATCAGTTACCAGCTCCCCC
VEGFA	F	CTGTCTAATGCCCTGGAGCC
	R	ACGCGAGTCTGTGTTTTTGC
PDGFA	F	GGGAACGCACCGAGGAAG
	R	GGAGGAGAAACAGGGAGTGC
PDGFB	F	GCTGAAAGGGTGGCAACTTC
	R	GGGAATGAAAAATGGGCGCT
ANG	F	TCCCGTTGAAGGGAAACTGC
	R	CCAGCACGAAGACCAACAAC
Internal control		
GAPDH	F	GAAAGCCTGCCGGTGACTAA
	R	AGGAAAAGCATCACCCGGAG

F, sequence of sense strands; R, sequence of anti-sense strands; IL6, interleukin-6; IL8, interleukin-8; IFNG, interferon gamma; TNF, tumor necrosis factor; FGF1, fibroblast growth factor-1; FGF2, fibroblast growth factor-2; VEGFA, vascular endothelial growth factor A; VEGFB, vascular endothelial growth factor B; PDGFA, platelet-derived growth factor subunit A; PDGFB, platelet-derived growth factor subunit B; ANG, angiopoietin

Table 2. Donor characteristics

Group	Number	Age (years)	Sex	Body mass index (kg/m^2)	Type of treatment
40s group	#1	45	Female	30.12	Depilation
	#2	47	Male	26.86	Rejuvenation
	#3	42	Male	27.32	Rejuvenation
60s group	#1	62	Male	25.46	Rejuvenation
	#2	62	Female	24.24	Arthritis
	#3	61	Female	32.00	Arthritis
Donor for characterization	#1	55	Male	25.78	Arthritis

multiple networks derived from different proteomic or genomic data sources and 2) the prediction of gene function.

Statistical analysis

All data were compared via one-way analysis of variance using the Statistical Package for the Social Sciences (SPSS, version 14.0K; SPSS Inc., Chicago, IL, USA). Data are expressed as mean $\pm$ standard error of the mean. Group means were considered significantly different at $p<0.05$, as determined by the protected least significant difference test when analysis of variance indicated an overall significant treatment effect ($p<0.05$).

Results

Characterization of human ADASs by passage

The 7 donors in this study were divided into 3 groups: >40 years of age (40s group, $n=3$), >60 years of age (60s group, $n=3$), and the characterization sample ($n=1$). The basic characteristics of the donors are shown in Table 2. To investigate the donor age-associated differences in ADASs isolated from human adipose tissue, ADASs were obtained from each of 3 donors in the 40s and 60s groups, characterized from 1 donor. ADASs isolated from human adipose tissue of donors in the 40s and 60s groups were

cultured until the number of cells had sufficiently increased (by passage 3) for co-culturing with HUVECs. Therefore, the surface marker expression of ADASs according to the passage number was first investigated using flow cytometry. No differences were observed in the first three passages of ADASs during characterization of ADASs in the subculture steps (Figure 1 and Table 1). Based on the results obtained during the characterization of the passages, the ADASs used in the current study expressed CD45, CD90, CD105, and CD106 but not CD31 or CD34 at passage 3 (Figure 1).

Determination of the concentration and treatment time of H_2O_2 in HUVECs

Analysis of the treatment duration and titration of H_2O_2 in HUVECs is necessary to evaluate the differential responses of HUVECs to isolated ADASs from donors of different ages under oxidative stress conditions. Accordingly, cell viability and ROS generation of HUVECs were measured using Ez-Cytox and DCF-DA with different concentrations of H_2O_2 (0–50 µM) and treatment times (0, 2, 4, or 6 h). Figure 2(a) shows the percentage of viable cells, and Figure 2(b) presents the number of ROS-generating HUVECs under oxidative stress conditions. HUVECs were most strongly affected by ROS generation when treated with 40 µM H_2O_2 for 4 h (Figure 2
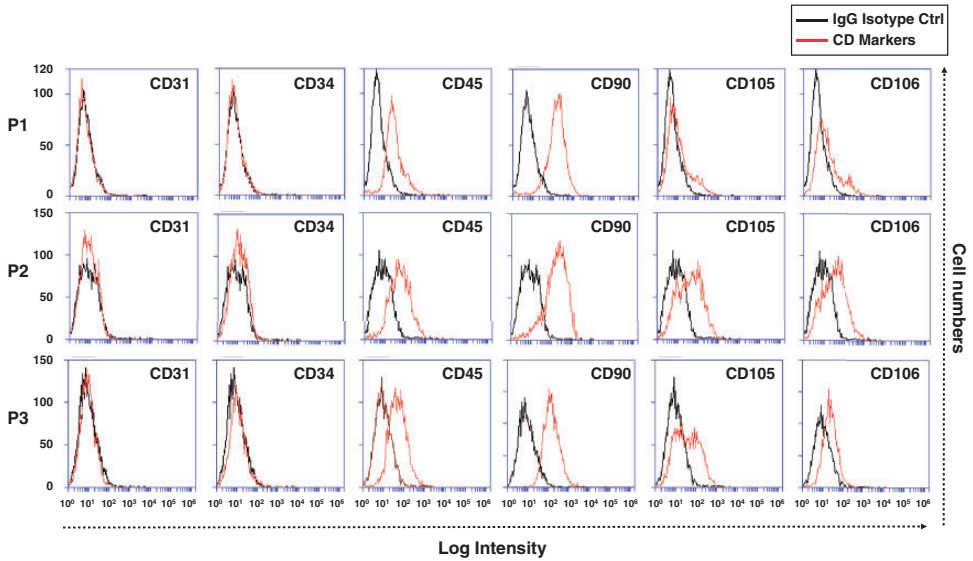
Figure 1. Surface marker expression on ADASs according to passage number as determined by flow cytometry. This figure shows the ADAS characterization results. The donor characteristics are summarized in Table 1.

ADASs, adipose-derived adherent stromal cells; P, passage.
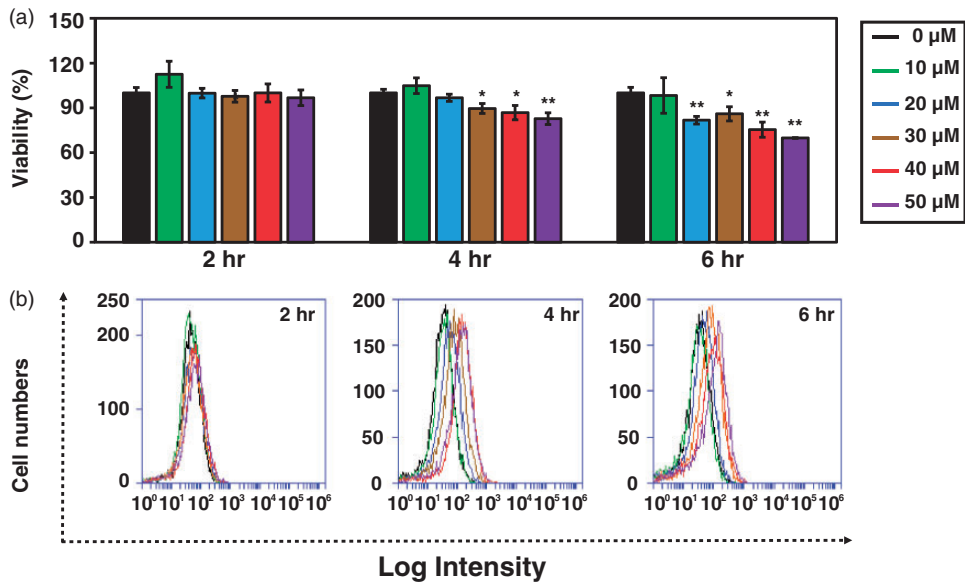
Figure 2. Cell viability and reactive oxygen species generation of human umbilical vein endothelial cells for various concentrations and times of H_2O_2 treatment. (a) Cell viability and (b) Reactive oxygen species generation were measured using Ez-Cytox and 2′,7′-dichlorofluorescein diacetate, respectively. Data are representative of three independent experiments. Significant differences between the untreated (0 µM) and H_2O_2-treated (10, 20, 30, 40, or 50 µM) groups were determined via analysis of variance. *$p<0.05$, **$p<0.01$.

Figure 3. Differential regulation of proteins related to anti-oxidant activity, apoptosis, inflammation, adhesion, and calcium regulation in human umbilical vein endothelial cells in respon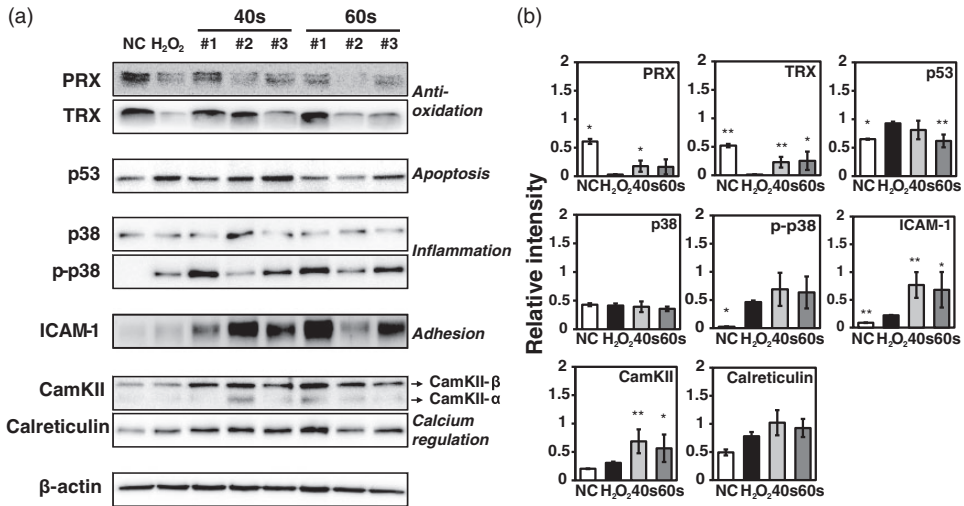se to adipose-derived adherent stromal cells and H_2O_2 treatment. (a) Differential regulation as determined via an immunoblot analysis. (b) Band intensity was measured as area density and analyzed by the ImageJ program. Relative intensity levels indicate protein levels normalized to β-actin levels. Data are representative of three independent experiments. Significant differences between the H_2O_2 treatment conditions in the negative control group and 40s and 60s groups were determined via analysis of variance. *$p < 0.05$, **$p < 0.01$.

(b)), although the cell viability was 87% at this concentration and treatment time (Figure 2(a)). Therefore, HUVECs were treated with 40 μM of H_2O_2 for 4 h in further studies.

Differential regulation of proteins related to anti-oxidant activity, apoptosis, inflammation, adhesion, and calcium regulation in HUVECs by ADASs

HUVECs pretreated with H_2O_2 were cultivated with ADASs isolated from human adipose tissue from both donor age groups (40s and 60s groups) for 48 h. The expression levels of proteins related to anti-oxidant activity, apoptosis, inflammation, adhesion, and calcium regulation in HUVECs were compared between the 40s and 60s groups using western blot analysis. The expression of anti-oxidant proteins [peroxiredoxin (PRX) and thioredoxin (TRX)]

in HUVECs was down-regulated by H_2O_2 but showed an upward trend in HUVECs co-cultured with ADASs (40s and 60s groups) (Figure 3). In contrast, the expression of HUVEC protein associated with apoptosis (p53) was increased by H_2O_2 but decreased in HUVECs co-cultured with ADASs despite variations among individuals (Figure 3). Moreover, proteins that are important for inflammation (phosphorylated p38), adhesion (intercellular adhesion molecule-1), and calcium regulation (Ca^{2+}/ calmodulin-dependent protein kinase II and calreticulin) exhibited a tendency to increase in H_2O_2-treated HUVECs and were more highly expressed in HUVECs co-cultured with ADASs than in H_2O_2-treated HUVECs (Figure 3). However, p38 was largely unchanged in all groups (Figure 3). Interestingly, little differences were observed in protein expression related to anti-oxidant activity, apoptosis, inflammation, adhesion,
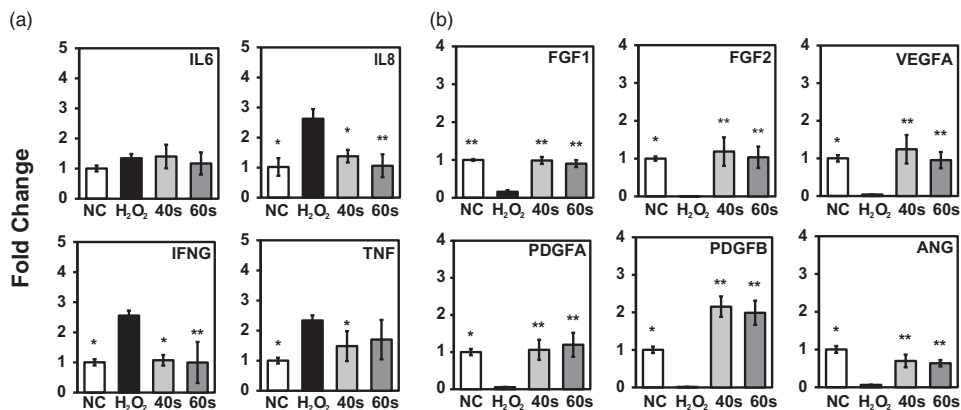
Figure 4. Gene expression related to (a) inflammation and (b) angiogenesis in human umbilical vein endothelial cells co-cultured with adipose-derived adherent stromal cells was determined via quantitative real-time polymerase chain reaction. Data are representative of three independent experiments. The transcript level of each gene was normalized to the GAPDH transcript levels. Significant differences between the H_2O_2 treatment conditions in the negative control group and 40s and 60s groups were determined by analysis of variance. $*p < 0.05$, $**p < 0.01$.

and calcium regulation between the 40s and 60s donors (Figure 3).

Gene expression related to inflammation and angiogenesis in HUVECs co-cultured with ADASs

H_2O_2-treated HUVECs were co-cultured with ADASs for 24 h, and the gene expression levels of pro-inflammatory cytokines [interleukin-6 (IL6), IL8, interferon gamma (IFNG), and tumor necrosis factor (TNF)] and angiogenic factors [fibroblast growth factor-1 (FGF1), FGF2, vascular endothelial growth factor A (VEGFA), platelet-derived growth factor subunit A (PDGFA), PDGFB, and angiopoietin (ANG)] were determined by qPCR. Consequently, IL8, IFNG, and TNF, but not IL6, were remarkably increased in H_2O_2-treated HUVECs but significantly decreased in HUVECs co-cultured with ADASs (Figure 4(a)). In addition, the expression of all monitored angiogenesis-related genes (*ANG*, *FGF1*, *FGF2*, *PDGFA*, *PDGFB*, and *VEGFA*) was dramatically increased by ADASs

(Figure 4(b)). Little differences were observed between the 40s and 60s donors (Figure 4).

Functional classification of differentially expressed proteins/genes by various bioinformatics resources

To determine the gene interactions for proteins/genes that were differentially altered in H_2O_2-treated HUVECs, 15 proteins/genes associated with anti-oxidation, apoptosis, inflammation, angiogenic factors, or calcium regulation were analyzed using GeneMANIA to determine the interactions of these proteins/genes [Figure 5(a)]. The 14 query genes (inside circle) and their interacting genes are presented in Figure 5(a). Function-based interactions with identified partners were predicted with genes associated with positive regulation of cell motility, cell migration, and the cellular components required for movement. Furthermore, identification of enriched functional gene groups using DAVID showed that the most strongly affected functional genes in ADASs were found in the Kyoto

Figure 5. Functional classification by various bioinformatics tools. (a) Networks from the GeneMANIA analysis showing the results of 15 queries (located inside the circle) and the function-based relationships. (b) Enriching the top term hit using DAVID identified cytokine–cytokine receptor interaction from the Kyoto Encyclopedia of Genes and Genomes pathway. Differentially expressed targets are marked with a red star on the figure.

Encyclopedia of Genes and Genomes pathway [Table 3 and Figure 5(b)]. Six of these genes (*CXCL8*, *IFNG*, *PDGFA*, *PDGFB*, *TNF*, and *VEGFA*) were localized to cytokine–cytokine receptor interaction and may play important roles in the development of new therapeutic strategies for various diseases using SVF transplantation.

Table 3. Target functional gene groups as identified by Functional Annotation Clustering

Category	Term	Count	p-value	Benjamini	FDR
KEGG_PATHWAY	Cytokine–cytokine receptor interaction	6	8.6×10^{-6}	3.6×10^{-4}	9.2×10^{-3}
KEGG_PATHWAY	Rheumatoid arthritis	5	4.9×10^{-6}	4.0×10^{-4}	5.2×10^{-3}
KEGG_PATHWAY	Malaria	4	3.9×10^{-5}	1.1×10^{-3}	4.2×10^{-2}
KEGG_PATHWAY	Pathways in cancer	6	1.2×10^{-4}	2.4×10^{-3}	1.2×10^{-1}
KEGG_PATHWAY	Melanoma	4	1.2×10^{-4}	2.0×10^{-3}	1.3×10^{-1}
KEGG_PATHWAY	Rap1 signaling pathway	5	1.5×10^{-4}	2.1×10^{-3}	1.6×10^{-1}
KEGG_PATHWAY	Ras signaling pathway	5	2.0×10^{-4}	2.4×10^{-3}	2.1×10^{-1}
KEGG_PATHWAY	MAPK signaling pathway	5	3.2×10^{-4}	3.3×10^{-3}	3.4×10^{-1}
KEGG_PATHWAY	HTLV-1 infection	5	3.2×10^{-4}	3.0×10^{-3}	3.5×10^{-1}
KEGG_PATHWAY	Chagas disease (American trypanosomiasis)	4	3.7×10^{-4}	3.1×10^{-3}	3.9×10^{-1}
KEGG_PATHWAY	African trypanosomiasis	3	9.7×10^{-4}	7.3×10^{-3}	1.0
KEGG_PATHWAY	PI3K-Akt signaling pathway	5	1.0×10^{-3}	7.0×10^{-3}	1.1
KEGG_PATHWAY	Influenza A	4	1.7×10^{-3}	1.1×10^{-2}	1.8
KEGG_PATHWAY	Regulation of actin cytoskeleton	4	2.9×10^{-3}	1.7×10^{-2}	3.0
KEGG_PATHWAY	Antigen processing and presentation	3	5.1×10^{-3}	2.8×10^{-2}	5.3
KEGG_PATHWAY	NF-kappa B signaling pathway	3	6.6×10^{-3}	3.4×10^{-2}	6.8
KEGG_PATHWAY	Amoebiasis	3	9.7×10^{-3}	4.6×10^{-2}	9.9
KEGG_PATHWAY	Natural killer cell-mediated cytotoxicity	3	1.3×10^{-2}	5.7×10^{-2}	13.0
KEGG_PATHWAY	Proteoglycans in cancer	3	3.2×10^{-2}	1.3×10^{-1}	30.0
KEGG_PATHWAY	Focal adhesion	3	3.4×10^{-2}	1.3×10^{-1}	31.0
KEGG_PATHWAY	Graft-versus-host disease	2	4.7×10^{-2}	1.7×10^{-1}	40.0
KEGG_PATHWAY	Allograft rejection	2	5.2×10^{-2}	1.8×10^{-1}	44.0

Benjamini, Benjamini–Hochberg critical value; FDR, false discovery rate; KEGG, Kyoto Encyclopedia of Genes and Genomes; MAPK, mitogen-activated protein kinase; HTLV-1, human T-lymphotropic virus 1; PI3K, phosphoinositide 3-kinase; Akt, protein kinase B; NF-kappa B, nuclear factor kappa B

Discussion

Adipose-derived SVFs contain pluripotent stem cells that can differentiate into osteogenic, adipogenic, myogenic, neurogenic, chondrogenic, and hematopoietic lineages.[22,23] Specifically, these cells spontaneously show a cardiomyocyte phenotype, which suggests that this phenotype may be required for differentiation in response to specific conditions.[5] Additionally, many reports have been published regarding the possibility of transplantation of adipose-derived SVFs as a therapy for heart disease.[3,6–8] Donor age is a critical factor in the regenerative capability of the cells in this cell-based therapy,[10–12] but controversial results have been observed in humans.[13–16] Our aim was to determine the effects of donor age on adipose-derived SVF transplantation into impaired heart tissue. Thus, we examined the effects of ADASs on HUVECs because endothelial cells are abundant in the heart,[17] and oxidative stress conditions were used as an environmental stimulus because of their critical role in many physiological processes in the heart.[18] Therefore, we explored the differential expression of proteins in endothelial cells co-cultured with adipose-derived ADASs from donors of different

ages (40s and 60s groups) under oxidative stress conditions (H_2O_2). Interestingly, although co-culturing HUVECs with ADASs ameliorated inflammation caused by an increase in oxidative stress conditions, few differences were observed between the ADASs from the 40s and 60s groups.

SVF cells are composed of heterogeneous cell populations including blood-derived cells (CD45$^+$), ASCs (CD31$^-$, CD34$^+$, CD45$^-$, CD90$^+$, CD105$^-$, and CD106$^+$), MSCs (CD31$^-$, CD34$^-$, CD45$^-$, CD90$^+$, CD105$^+$, and CD106$^+$), endothelial (progenitor) cells (CD31$^+$, CD34$^+$, CD45$^-$, CD90$^+$, CD105$^-$, and CD106$^+$), vascular smooth muscle cells (CD31$^-$, CD34$^+$, CD45$^-$, CD90$^+$, CD105$^-$, and CD106$^-$), pericytes (CD31$^-$, CD34$^-$, CD45$^-$, CD90$^+$, CD105$^-$, and CD106$^+$), and other cells.[4,23,24] Differences exist in the phenotype and kinetics of differentiation between freshly isolated SVFs and cultured ADASs.[24,25] However, by passage 3, the differences in surface marker expression of cultured ADASs were negligible (Figure 1). In addition, the ADASs used in our study expressed CD45, CD90, CD105, and CD106 but neither CD31 nor CD34 (Figure 1). After plastic adherent culture, CD45 in ADASs is usually almost absent.[26] Interestingly, the expanded ADASs used in the present study expressed CD45 by passage 3 (Figure 1). The most likely reasons for this are the method used for isolation of SVFs,[27] the short period of time for adherent culture, and the increased numbers of adherent leukocytes in patients with arthritis[28] (Table 1). These factors may make CD45 expression possible in cultured and expanded ADASs. In this study, we used cultured ADASs from passage 3 to ensure that sufficient numbers of ADASs were available for co-culturing with HUVECs.

Prior to the beginning of this study, we anticipated that anti-oxidant proteins would be down-regulated and that proteins related to apoptosis, inflammation, adhesion, and calcium regulation would be up-regulated in H_2O_2-treated HUVECs. We also predicted that these proteins would show opposite expression patterns when exposed to ADASs compared with H_2O_2 treatment. Consistent with our expectations, the expression levels of most proteins were altered in HUVECs treated with H_2O_2 (Figure 3 and Figure 4). However, contrary to our expectations, proteins other than anti-oxidant proteins and apoptosis-related proteins were up-regulated to a greater extent in cells exposed to ADASs than in the H_2O_2-treated HUVECs (Figure 3).

Oxidative stress is characterized by elevated intracellular ROS that damage lipids, proteins, and DNA, and numerous metabolic, structural, and functional effects due to oxidative stress have been observed in many experimental and clinical investigations.[29] The defense mechanisms against oxidative stress include (enzymatic) anti-oxidant defenses such as superoxide dismutases, glutathione peroxidases, catalases, PRX, and TRX.[26] Moreover, oxidative stress induces p53 activation and apoptotic induction.[29] Consistent with previous reports,[26,29] anti-oxidant proteins (PRX and TRX) were down-regulated in HUVECs by H_2O_2 and enhanced by treatment of ADASs, although individual variations were observed. However, p53 was increased by H_2O_2 and decreased by ADASs (Figure 3). These results imply that proteins and/or extracellular vesicles secreted in response to ADASs may induce enzymatic anti-oxidant defenses and/or anti-apoptotic signals in endothelial cells.

We assumed that proteins showing reverse trends in expression in response to ADASs were affected by pro-inflammatory cytokines through paracrine and/or autocrine reactions[8]; however, some genes were

decreased by co-culturing HUVECs with ADASs (Figure 4(a)). Angiogenesis is a therapeutic target for the treatment of cardiovascular disease,[8] and some proteins show opposite expression patterns during angiogenesis.[30] We also observed that angiogenic factors were remarkably increased by co-culturing HUVECs with ADASs (Figure 4(a)). These results suggest that ADASs may induce angiogenesis and anti-inflammation in endothelial cells and contribute to restoration in patients with cardiac failure. Despite the controversial results regarding donor age with respect to SVF transplantation,[11–17] we showed very little difference in the expression of proteins between donors in the 40s and 60s groups under oxidative stress conditions (Figure 3 and Figure 4). In the functional analysis by GeneMANIA, enriched functional-related gene groups were predicted with 14 genes associated with positive regulation of cell motility, cell migration, and cell component movement in functional features. Furthermore, the most strongly affected functional genes (CXCL8, IFNG, PDGFA, PDGFB, TNF, and VEGFA) were those associated with cytokine–cytokine receptor interaction based on the DAVID enrichment analysis and may play important roles in the development of new therapeutic strategies for various diseases.

This study has shown that the profiles of proteins expressed in HUVECs in response to isolated ADASs exhibit few differences according to donor age under oxidative stress conditions. We expect that these results will provide the basis for the clinical application of SVF transplantation into impaired heart tissue. However, further studies using more donors with diverse ages, various environmental conditions, and varied target proteins are required for a better understanding of the influences of age on human ADASs.

Declaration of conflicting interest

Funding

References

1. Nguyen A, Guo J, Banyard DA, et al. Stromal vascular fraction: A regenerative reality? Part 1: Current concepts and review of the literature. *J Plast Reconstr Aesthet Surg* 2016; 69: 170–179.
2. Guo J, Nguyen A, Banyard DA, et al. Stromal vascular fraction: A regenerative reality? Part 2: Mechanisms of regenerative action. *J Plast Reconstr Aesthet Surg* 2016; 69: 180–188.
3. Alt E, Pinkernell K, Scharlau M, et al. Effect of freshly isolated autologous tissue resident stromal cells on cardiac function and perfusion following acute myocardial infarction. *Int J Cardiol* 2010; 144: 26–35.
4. Lin K, Matsubara Y, Masuda Y, et al. Characterization of adipose tissue-derived cells isolated with the Celution system. *Cytotherapy* 2008; 10: 417–426.
5. Planat-Benard V, Menard C, Andre M, et al. Spontaneous cardiomyocyte differentiation from adipose tissue stroma cells. *Circ Res* 2004; 94: 223–229.
6. Leblanc AJ, Nguyen QT, Touroo JS, et al. Adipose-derived cell construct stabilizes heart function and increases microvascular perfusion in an established infarct. *Stem Cells Transl Med* 2013; 2: 896–905.
7. Mazo M, Cemborain A, Gavira JJ, et al. Adipose stromal vascular fraction improves cardiac function in chronic myocardial infarction through differentiation and paracrine activity. *Cell Transplant* 2012; 21: 1023–1037.
8. Premaratne GU, Ma LP, Fujita M, et al. Stromal vascular fraction transplantation as an alternative therapy for ischemic

heart failure: anti-inflammatory role. *J Cardiothorac Surg* 2011; 6: 43.

9. Han S, Sun HM, Hwang KC, et al. Adipose-derived stromal vascular fraction cells: update on clinical utility and efficacy. *Crit Rev Eukaryot Gene Expr* 2015; 25: 145–152.

10. Alt EU, Senst C, Murthy SN, et al. Aging alters tissue resident mesenchymal stem cell properties. *Stem Cell Res* 2012; 8: 215–225.

11. Madonna R, Renna FV, Cellini C, et al. Age-dependent impairment of number and angiogenic potential of adipose tissue-derived progenitor cells. *Eur J Clin Invest* 2011; 41: 126–133.

12. Dos-Anjos Vilaboa S, Navarro-Palou M and Llull R. Age influence on stromal vascular fraction cell yield obtained from human lipoaspirates. *Cytotherapy* 2014; 16: 1092–1097.

13. de Girolamo L, Lopa S, Arrigoni E, et al. Human adipose-derived stem cells isolated from young and elderly women: their differentiation potential and scaffold interaction during in vitro osteoblastic differentiation. *Cytotherapy* 2009; 11: 793–803.

14. Aust L, Devlin B, Foster SJ, et al. Yield of human adipose-derived adult stem cells from liposuction aspirates. *Cytotherapy* 2004; 6: 7–14.

15. Ding DC, Chou HL, Hung WT, et al. Human adipose-derived stem cells cultured in keratinocyte serum free medium: Donor's age does not affect the proliferation and differentiation capacities. *J Biomed Sci* 2013; 20: 59.

16. Rodriguez JP, Murphy MP, Hong S, et al. Autologous stromal vascular fraction therapy for rheumatoid arthritis: rationale and clinical safety. *Int Arch Med* 2012; 5: 5.

17. Tirziu D, Giordano FJ and Simons M. Cell communications in the heart. *Circulation* 2010; 122: 928–937.

18. Burgoyne JR, Mongue-Din H, Eaton P, et al. Redox signaling in cardiac physiology and pathology. *Circ Res* 2012; 111: 1091–1106.

19. Kim SW, Choi JW, Lee DS, et al. Sex hormones regulate hepatic fetuin expression in male and female rats. *Cell Physiol Biochem* 2014; 34: 554–564.

20. Huang da W, Sherman BT and Lempicki RA. Systematic and integrative analysis of large gene lists using DAVID bioinformatics resources. *Nat Protoc* 2009; 4: 44–57.

21. Vlasblom J, Zuberi K, Rodriguez H, et al. Novel function discovery with GeneMANIA: a new integrated resource for gene function prediction in *Escherichia coli*. *Bioinformatics* 2015; 31: 306–310.

22. Cousin B, Andre M, Arnaud E, et al. Reconstitution of lethally irradiated mice by cells isolated from adipose tissue. *Biochem Biophys Res Commun* 2003; 301: 1016–1022.

23. Zuk PA, Zhu M, Ashjian P, et al. Human adipose tissue is a source of multipotent stem cells. *Mol Biol Cell* 2002; 13: 4279–4295.

24. Yoshimura K, Shigeura T, Matsumoto D, et al. Characterization of freshly isolated and cultured cells derived from the fatty and fluid portions of liposuction aspirates. *J Cell Physiol* 2006; 208: 64–76.

25. Varma MJ, Breuls RG, Schouten TE, et al. Phenotypical and functional characterization of freshly isolated adipose tissue-derived stem cells. *Stem Cells Dev* 2007; 16: 91–104.

26. Elisa M, Barbara B, Enrico R, et al. Defining the identity of human adipose-derived mesenchymal stem cells. *Biochem Cell Biol* 2015; 93: 1–9.

27. Bora P and Majumdar AS. Adipose tissue-derived stromal vascular fraction in regenerative medicine: A brief review on biology and translation. *Stem Cell Res Ther* 2017; 8: 145.

28. Szekanecz Z and Koch AE. Cell-cell interactions in synovitis. Endothelial cells and immune cell migration. *Arthritis Res* 2000; 2: 368–373.

29. Rochette L, Lorin J, Zeller M, et al. Nitric oxide synthase inhibition and oxidative stress in cardiovascular diseases: possible therapeutic targets? *Pharmacol Ther* 2013; 140: 239–257.

30. Park JY, Kim BS and Lee J. Evaluation of the angiogenic potency of a novel exopolysaccharide produced by the MK1 bacterial strain. *Arch Pharm Res* 2016; 39: 1223–1231.